SMA Polymer Thin Film Electrodeposition on Carbon Particles

V. M. DESAI,* R. MAHALINGAM,*,† and R. V. SUBRAMANIAN‡

*Department of Chemical Engineering and ‡Department of Mechanical and Materials Engineering, Washington State University, Pullman, Washington 99164-2710

SYNOPSIS

Electrodeposition of styrene-*co*-maleic anhydride (SMA) polymer, as thin films on carbon particle substrates, was carried out in a fluidized electrode bed reactor (FEBR). Feeder current, time of deposition, flow rate of anolyte (i.e., bed expansion or bed porosity), concentration of SMA in the anolyte, and pH of the anolyte were the key parameters investigated. The film characteristics were evaluated through SEM and FTIR analyses, the amounts determined by weighing. The effect of these parameters on the electrodeposition process is discussed and optimum conditions for deposition are proposed. Also, a possible mechanism for electrodeposition, particularly for the SMA–carbon system, is discussed. Furthermore, where relevant, the parameters and mechanism are compared with those for our parallel work on the ethylene-*co*-acrylic acid (EAA)–carbon system.

INTRODUCTION

Electrode reactions are traditionally carried out in stationary cells, for metals recovery. In our on-going research program, electropolymerization is investigated in a fluidized electrode bed reactor (FEBR). FEBR gives the following important advantages over a stationary cell:

1. High mass transfer rates due to the continuous disturbance of the diffusion boundary layer caused by particle collisions and turbulence.
2. Low current densities favorable for electroorganic reactions.
3. Large electrode surface area per unit electrode volume.
4. Uniform coating of film on the surface.

Our previous work on the FEBR is described in Refs. 1–6 and our recent parallel work on EAA polymer is described in Refs. 7 and 8.

† To whom correspondence should be addressed.

Journal of Applied Polymer Science, Vol. 44, 29–40 (1992)
 CCC 0021-8995/92/010029-12$04.00

EXPERIMENTAL

Materials Preparation

The experiments used a bed of graphite particles as the working electrode, the anode, and a graphite rod as the current feeder, both prepared as described in Refs. 7 and 8. SMA powder used in the preparation of SMA solution was SMA 1000A resin supplied by the Sartomer Co. and had a specific gravity of 1.34 and a molecular weight of 1600. The copolymer consisted of a 1 : 1 mixture of styrene and maleic anhydride.

Experimental

The FEBR, the power supply unit, the flow diagram and the run operating procedure are described in Refs. 7 and 8. Both the anolyte and catholyte were 2000 mL of the same EAA solution maintained at the same concentration of 5 wt % and same pH of 3.0 for all the experiments, except wherein the concentration or pH was varied as a parameter. The SMA solution was prepared by dissolving 100 g of SMA 1000A powder in 2000 mL of water. The SMA as such is insoluble in water and hence, in order to dissolve it, about 6 mL of ammonium hydroxide were added, while heating and stirring the solution. pH

was maintained at an approximate minimum value of 3.0 by ammonium hydroxide addition.

The first parameter investigated was the feeder current, the experiments being performed at a constant feeder current. In the case of SMA, the feeder current was varied as a parameter from 0.05 to 0.5 A, at a bed expansion of 22.2% and a corresponding bed porosity of 0.648 (at an anolyte flow rate of 25 mL/s). Next, the effect of deposition time on polymer deposition was investigated. The time was varied from 1 min to a maximum of 8 min. This also was done at a bed expansion of 22.2%. The feeder current was maintained constant at 0.2 A for each experiment. The third parameter investigated was the anolyte flow rate (i.e., effect of bed expansion or bed porosity) on polymer deposition. Experiments were carried out for no-flow condition (i.e., stationary bed) as also for flow rate variations from 8.33 to 41.33 mL/s. Incipient fluidization was observed at 16.7 mL/s. These experiments were carried out at a 0.2 A feeder current and for a deposition period of 3 min. Concentration of SMA solution was next studied as a parameter, in the range 2.5–10 wt %. This was done at a feeder current of 0.2 A, a time of deposition of 3 min, a bed expansion of 22.2%, and an anolyte pH of 3.0. The concentration was varied by adding appropriate amounts of SMA 1000A powder in water and dissolving it by adding minimal amounts of ammonium hydroxide in water to maintain a pH of approximately 3.0. Finally, the effect of pH on deposition of polymer was examined. The experiments were carried out at a feeder current of 0.2 A, time of deposition of 3 min, bed expansion of 22.2%, and 5 wt % concentration of anolyte SMA solution. The pH was varied from 3.0 to 8.8 by adding appropriate amounts of ammonium hydroxide to the SMA solution.

Evaluation of Polymer Deposits

The amount of polymer deposited on the particles and on the current feeder was measured by weighing. A scanning electron microscope, Hitachi S-570, was used to study changes in both thickness and surface morphology, by examining a representative particle from each experimental run. Fourier transform infrared (FTIR) spectroscopy studies were carried out on the deposited films, on a Nicolet 5DX unit. Full details are available in Refs. 7 and 8.

RESULTS AND DISCUSSION

Effect of Feeder Current

The experiments were carried out at constant feeder currents, ranging from 0.05 to 0.5 A. A constant bed

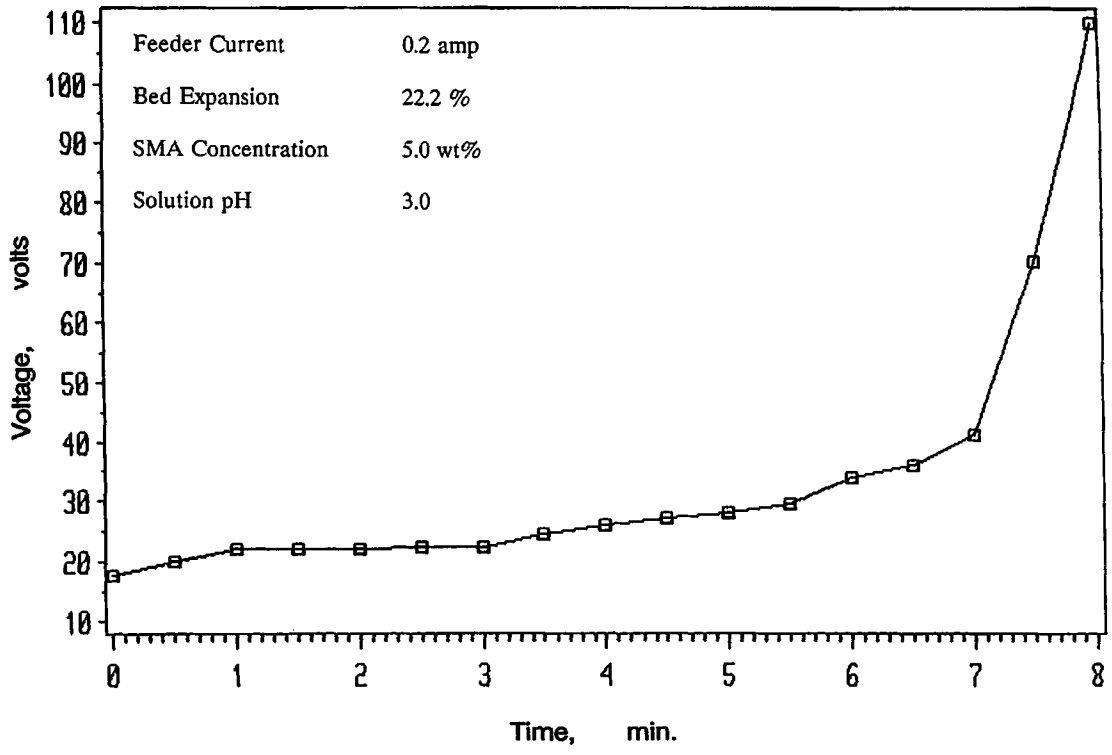

Figure 1 Variation of voltage with time.

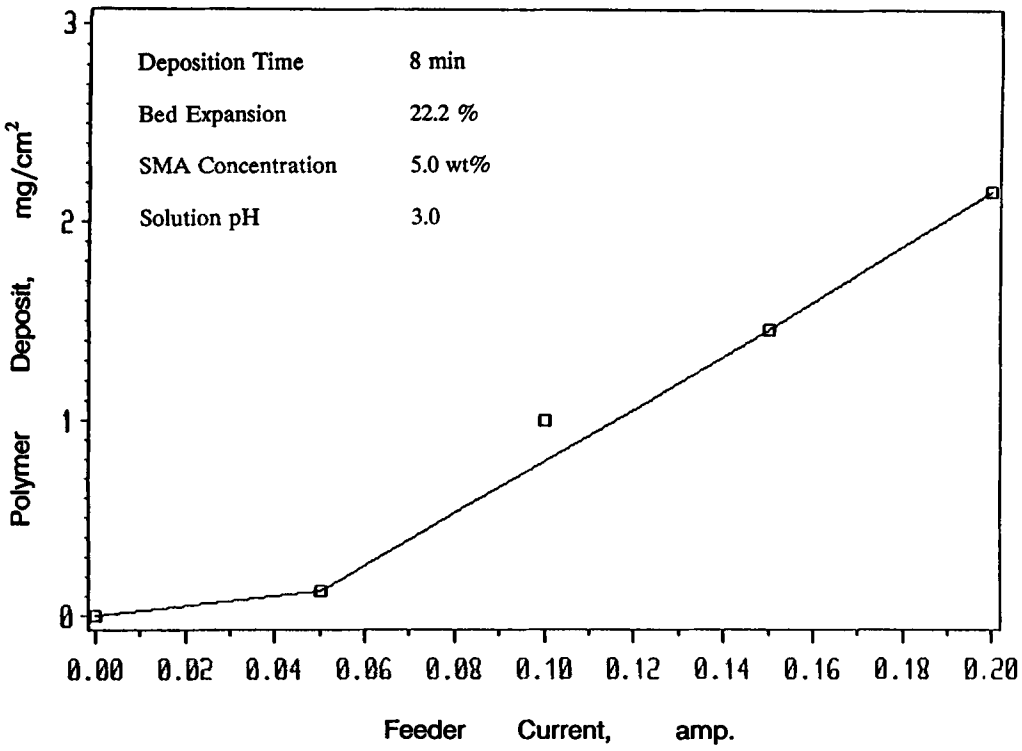

Figure 2(a) Effect of feeder current on SMA polymer deposition.

expansion of around 22.2% was used for these runs. Over this range of feeder currents, a deposition run time of 8 min was found feasible. The run time declined at higher feeder currents. This was due to the nonconductive nature of the polymer deposit. Electrodeposition of the polymer on the current feeder and graphite particles decreased the substrate conductivities, thus increasing the resistance to the flow of electrons. Thus, the voltage required to maintain the current constant had to be increased with time. For lower currents, it was possible to carry out the process up to an average approximate time of 8 min during which time the resistance of the cell was constantly building up. Beyond 8 min, the resistance of the cell had built up to such an extent that even a maximum applied voltage of 340 V could not support the current. At this point, the current began to decline rapidly and the run was terminated. A representative variation of voltage with time at a feeder current of 0.2 A is shown in Figure 1.

Figure 2(a) shows a plot of polymer deposit versus feeder current. It can be seen that at 0.05 A hardly any polymer deposit is obtained. This is because the current is insufficient to sustain electrodeposition. Beyond this, the polymer deposit varies linearly with feeder current up to 0.2 A. Polymer deposition does occur for a feeder current of 0.3 A (not shown); however, at higher feeder currents of 0.4 and 0.5 A, the run time is too small to give any significant deposition.

Figure 2(b) shows the SEM pictures of polymer films at feeder currents of 0.05, 0.1, 0.15, and 0.2 A. At 0.05 A, there is hardly any film growth on the particles and the bare graphite surface is seen. At 0.1 A a very thin film is formed on the surface of the particles. At 0.15 A and higher, a gradual increase in film growth is seen on the particles. At 0.2 A, however, the film thickness is highest. This indicates that at a feeder current of 0.2 A, the polymer deposit is maximum. Hence, 0.2 A is chosen as the optimum feeder current for all subsequent experiments with SMA.

Effect of Deposition Time

The kinetics of film growth were next evaluated at the constant optimum feeder current of 0.2 A described in the previous graph. The bed expansion was again maintained at 22.2%. Run time was varied from 1 to 8 min. Figure 3(a) shows the increase in polymer deposit with time. An initial induction period of 1 min was observed during which very little polymer deposit is obtained. After this, a rapid increase is seen till about 3 min, beyond which the deposition rate rises only slowly. Next, the SMA polymer deposit versus time in Figure 3(a) is re-

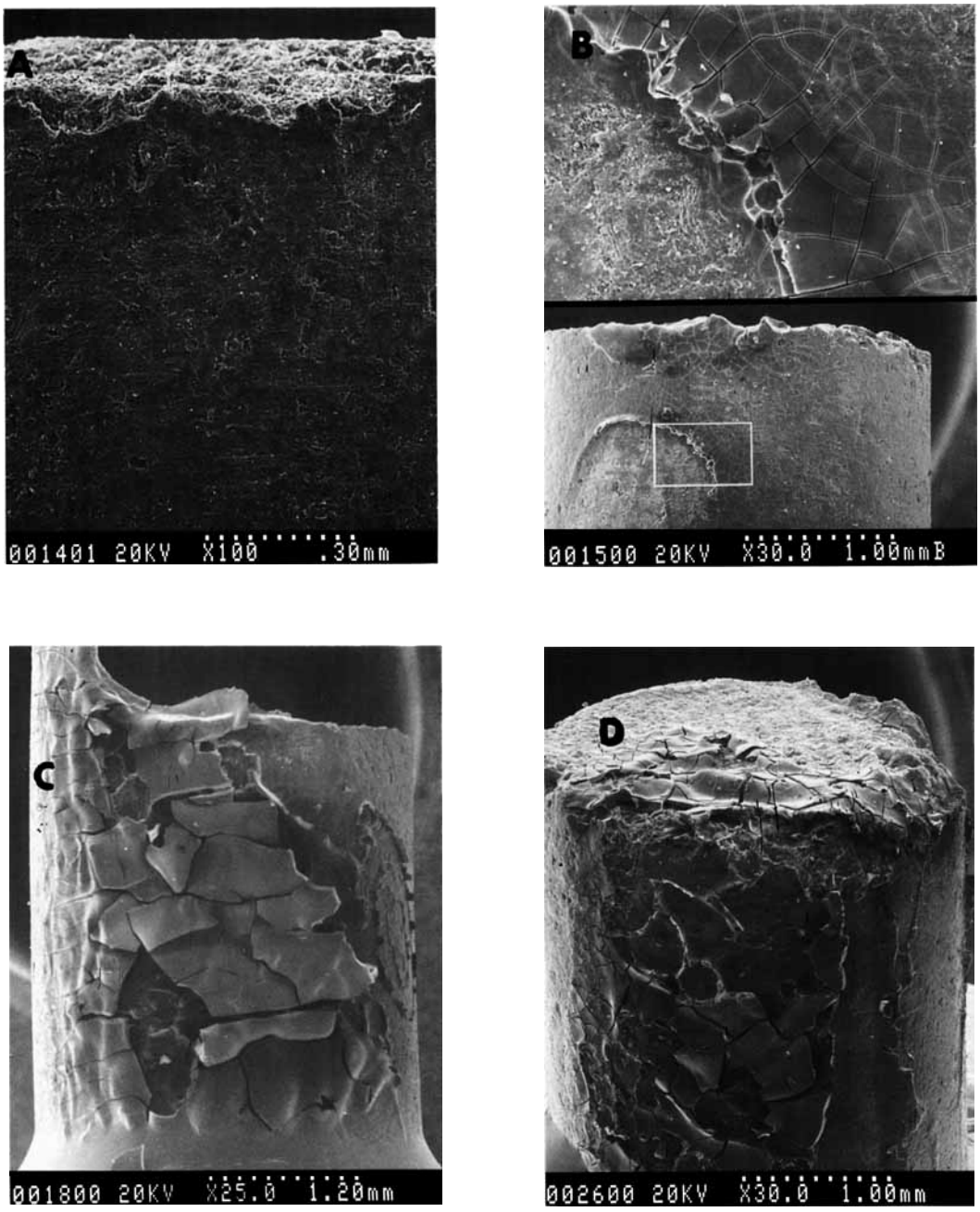

Figure 2(b) SEM pictures showing effect of feeder current on SMA polymer deposition. Feeder current (A), magnification: (A) 0.05, 100×; (B) 0.10, 30×; (C) 0.15, 25×; (D) 0.20, 30×.

plotted versus the square root of time,[9] as shown in Figure 3(b). In Figure 3(a), the rapid polymer deposit till about 3 min is considered the nucleation phase. Olson[10] has suggested that this is the unimpeded growth of the film in the initial stages. Next, beyond 3 min, the polymer deposition is in the slow growth phase, due to diffusional resistance encountered; such a process, as to be expected, exhibiting linearity with square root of time, as in Figure 3(b). The reason for the occurrence of both rapid nucleation growth and slow diffusional growth phases for SMA films is explained in a later section, with the help of a mechanism postulated for electrodeposition. Such a two-step growth is not seen in the case of EAA [see Fig. 3(a), Ref. 8]. Figure 3(c) shows SEM pictures of SMA polymer deposits at deposi-

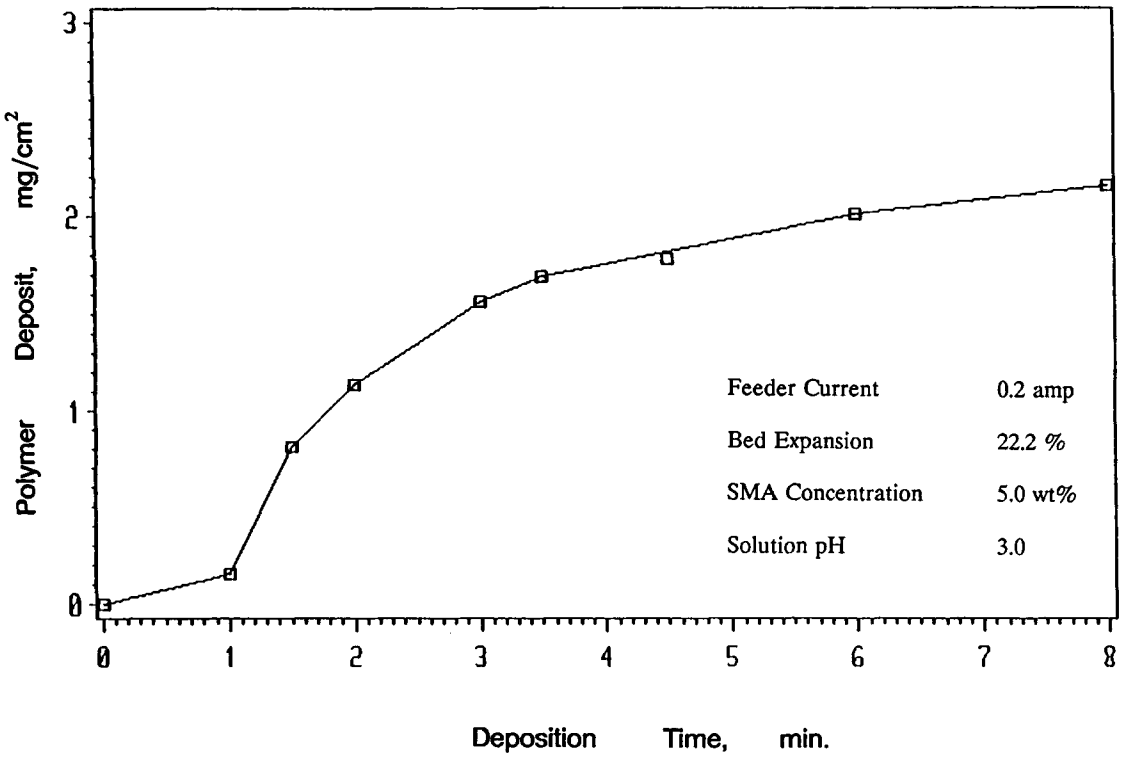

Figure 3(a) Kinetics of SMA polymer deposition.

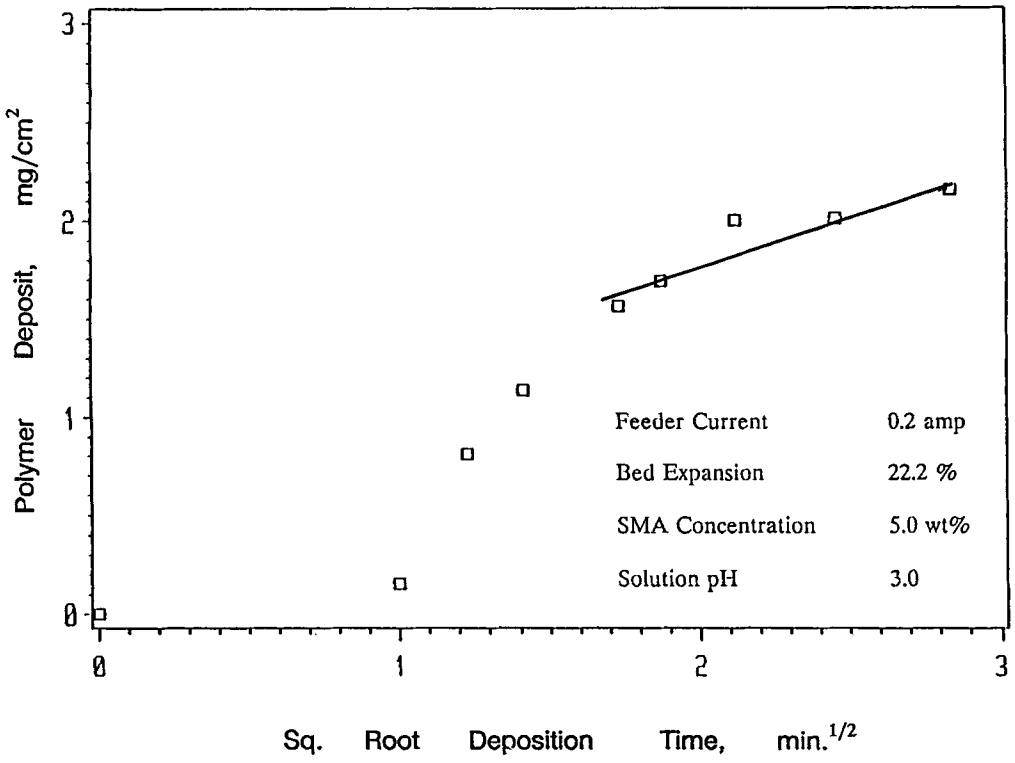

Figure 3(b) Variation of SMA polymer deposit with square root of time.

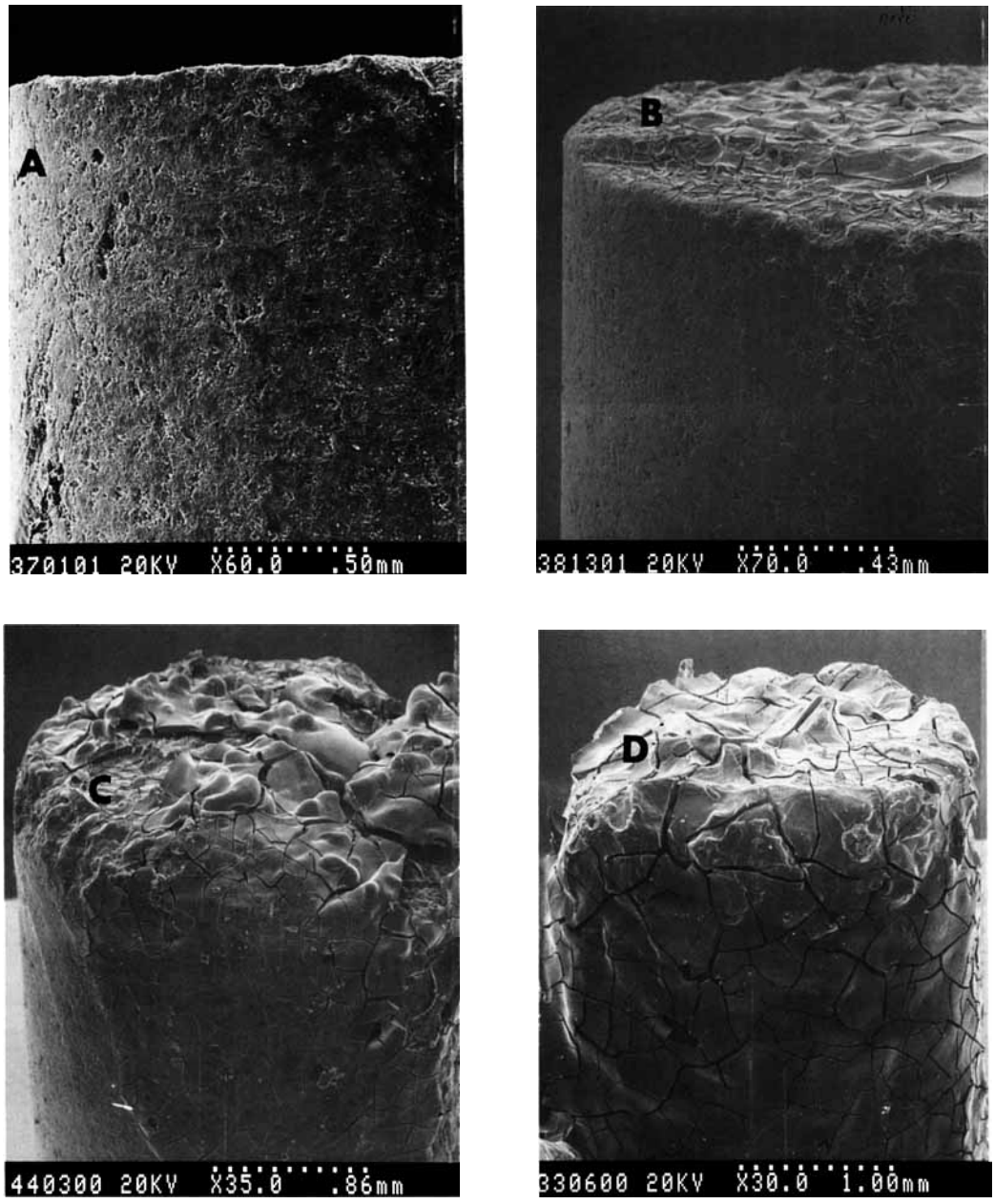

Figure 3(c) SEM pictures on kinetics of SMA polymer deposition. Time (min), magnification: (A) 1.0, 60×; (B) 1.5, 70×; (C) 3.0, 35×; (D) 6.0, 30×.

tion times of 1, 1.5, 3, and 6 min. At 1 min, hardly any polymer deposit is seen, corresponding to the induction period. At 3 min, a thin layer is seen while, at 6 min, growth over the entire particle surface is seen.

Effect of Anolyte Flow Rate

The variation of SMA polymer deposition with flow rate is shown in Figure 4. Two peaks were observed, one at incipient fluidization and the other at around 22.2% bed expansion (bed porosity of 0.648). The observations in Fig. 4 are explained as follows. When the bed is stationary, the entire surface area of the particles is not available for deposition. This leads to lower polymer deposition values. As the flow rate is increased, more and more surface becomes available for polymer deposition through increase in bed porosity, thus leading to increased polymer deposition. This trend is seen till incipient fluidization.

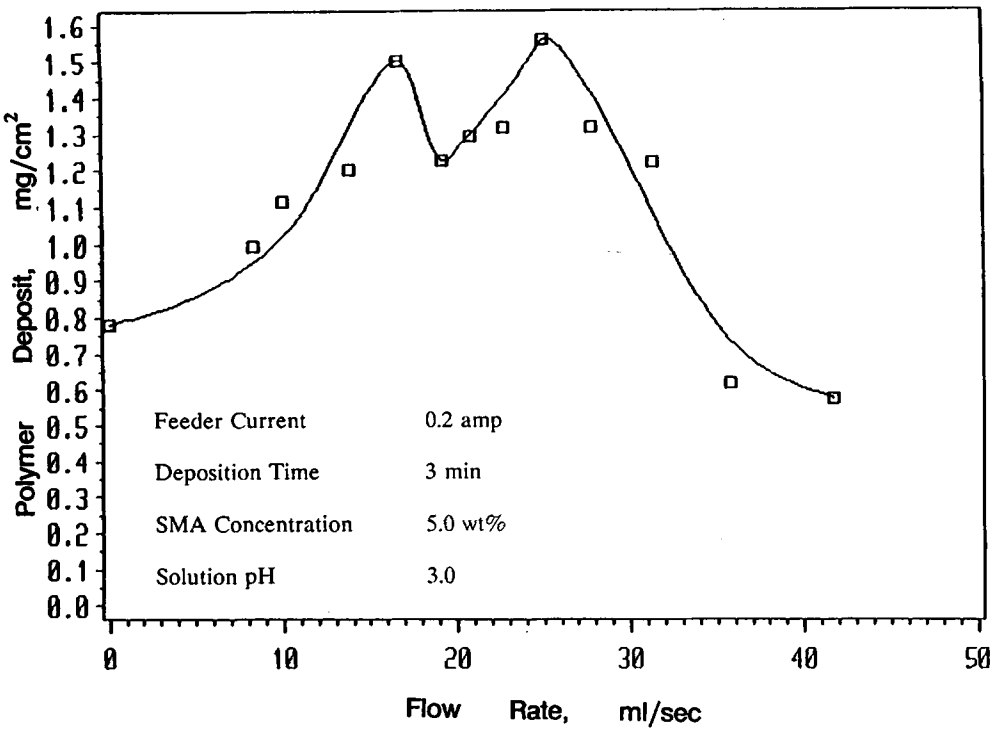

Figure 4 Effect of anolyte flow rate on SMA polymer deposition.

At incipient fluidization, there is still no bed expansion but it is a point at which fluidization does begin. At this point, practically the entire surface of the particles becomes available for deposition. Hence, the polymer deposition is maximum at this point.

The polymer deposition starts declining after this

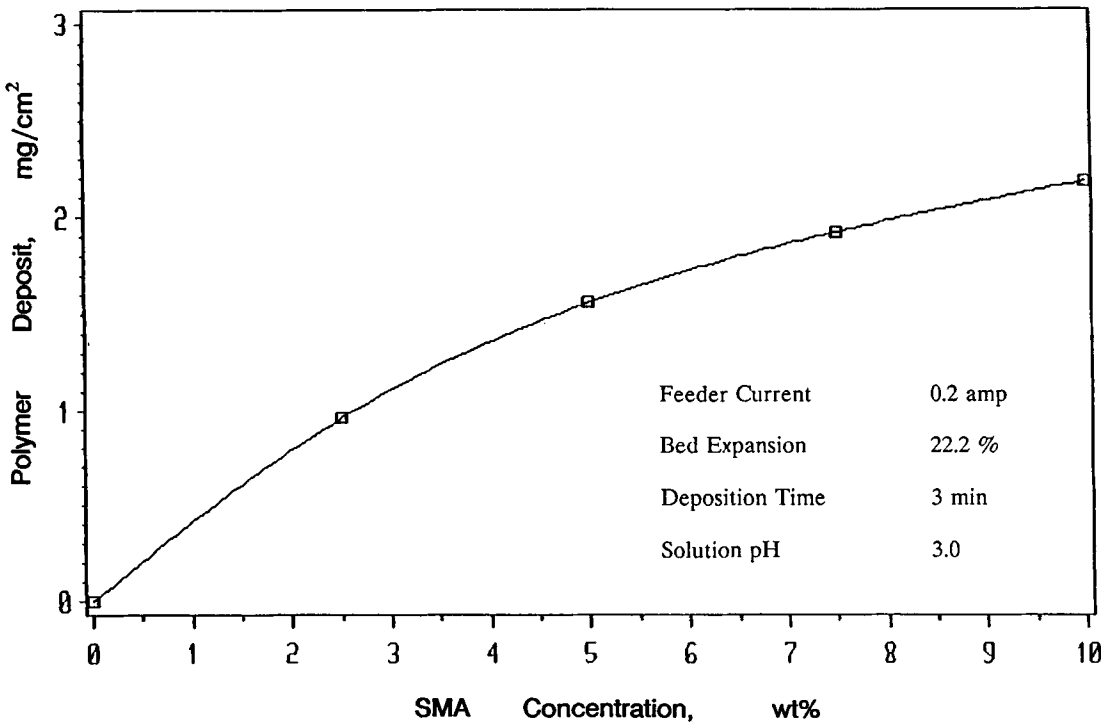

Figure 5(a) Effect of SMA concentration on SMA polymer deposition.

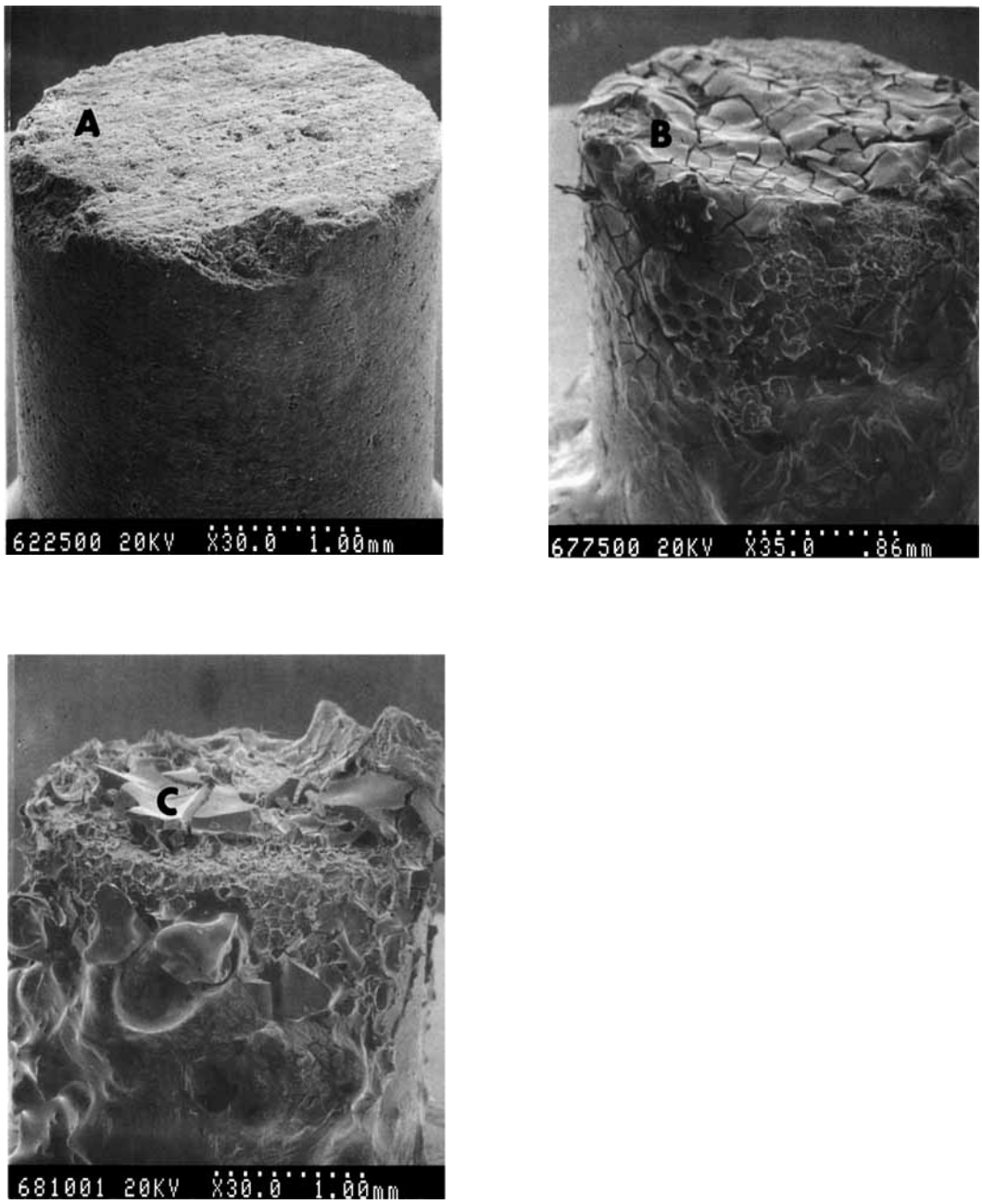

Figure 5 (b) SEM pictures showing effect of SMA concentration on polymer deposition. Concentration (wt %), magnification: (A) 2.50, 30×; (B) 7.50, 35×; (C) 10.00, 30×.

point. This is because, as the flow rate increases past the incipient fluidization state, the contact between the particles is broken. As the flow rate is increased further, both the mass transfer rates as well as the separation between particles increase. These two competing mechanisms have opposing effects on polymer deposition, the former favoring an increase in polymer deposition and the latter favoring a decrease. In this region, at lower flow rates, however, the separation between the particles is not very high; thus, mass transfer effects predominate, leading to an increase in polymer deposition and giving rise to the second peak. This second peak is seen at a flow rate of 25 mL/s, i.e., at a bed expansion of around 22.5%. At higher flow rates, however, the separation between particles predominates, this

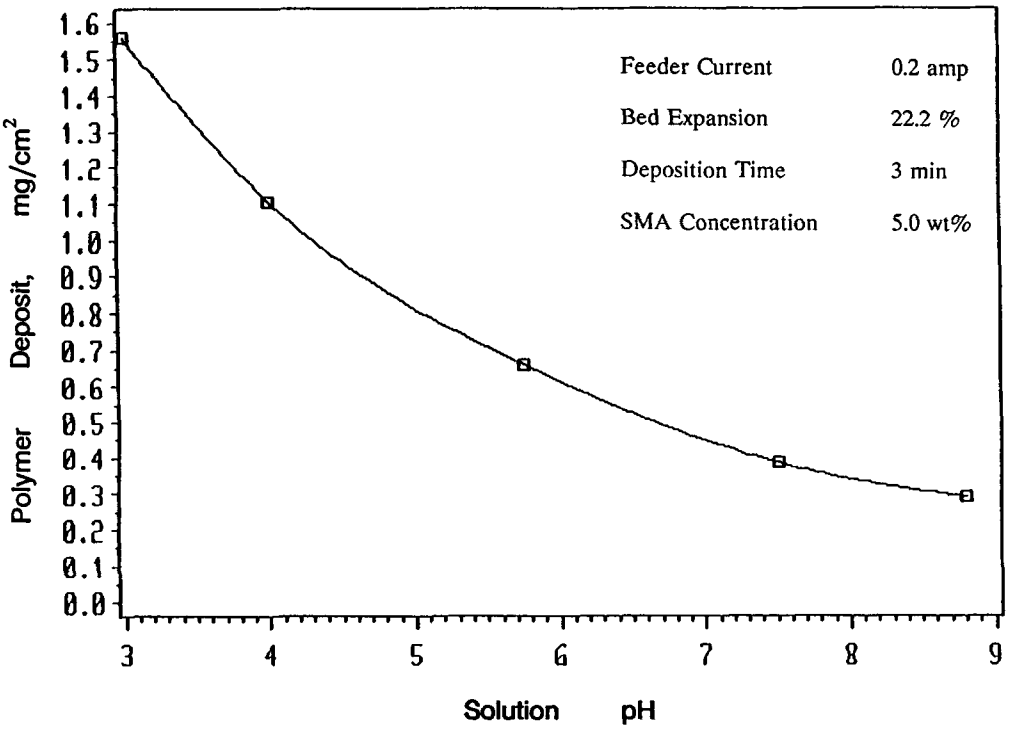

Figure 6(a) Effect of solution pH on SMA polymer deposition.

again leading to a decrease in polymer deposition. A similar behavior is observed in the case of EAA also.[8]

Effect of Anolyte SMA Concentration

Concentration of SMA was next varied from 2.5 to 10 wt % and its effect on polymer deposition is shown in Figure 5(a). The SEM pictures of polymer films for some selected concentrations are shown in Figure 5(b); the film is seen to be quite thick at higher concentrations.

Effect of Solution pH

Referring to Figure 6(a), maximum deposition is obtained at the acidic pH of 3.0. As the pH is increased, the polymer deposition, however, decreases. This is due to the SMA coating redissolving in ammonium hydroxide, added to increase the pH. The SMA pictures are shown in Figure 6(b). It can be seen the film gets thinner as the pH increases.

Mechanism for Electrodeposition of SMA

The mechanism for electrodeposition of SMA is illustrated in Figure 7. In aqueous ammonium solutions, SMA exist as ions. During electrolysis, passage of current through an electrode–solution interface causes chemical changes or migration of ions. When electrolysis begins, the hydrogen ion concentration in the immediate vicinity of the anode will be high. Due to this, the polymer forms an insoluble acid and precipitates out of the solution onto the surface of the anode. In SMA, however, there are two carboxylic acid groups and hence there is elimination of water to form the anhydride in the direct deposition of SMA as acid on the anode surface. As soon as the first layer of deposit is formed on the current feeder and the graphite particles, the movement of hydrogen ions is restricted and can now occur only through the pores of the film. The SMA polymer, however, appears to have poorer film integrity, compared to EAA[8]; this is due to the molecular weight of the SMA polymer being low, only around 1600. Furthermore, the elimination of water in the deposition mechanism results in cracks and pores in the film. Additional factors to consider are mechanical compaction of the film after deposition and electroosmosis. The pores and cracks allow the flow of hydrogen ions for a period even beyond that for the formation of first layer of film, hence increased deposits unlike that for EAA.[8]

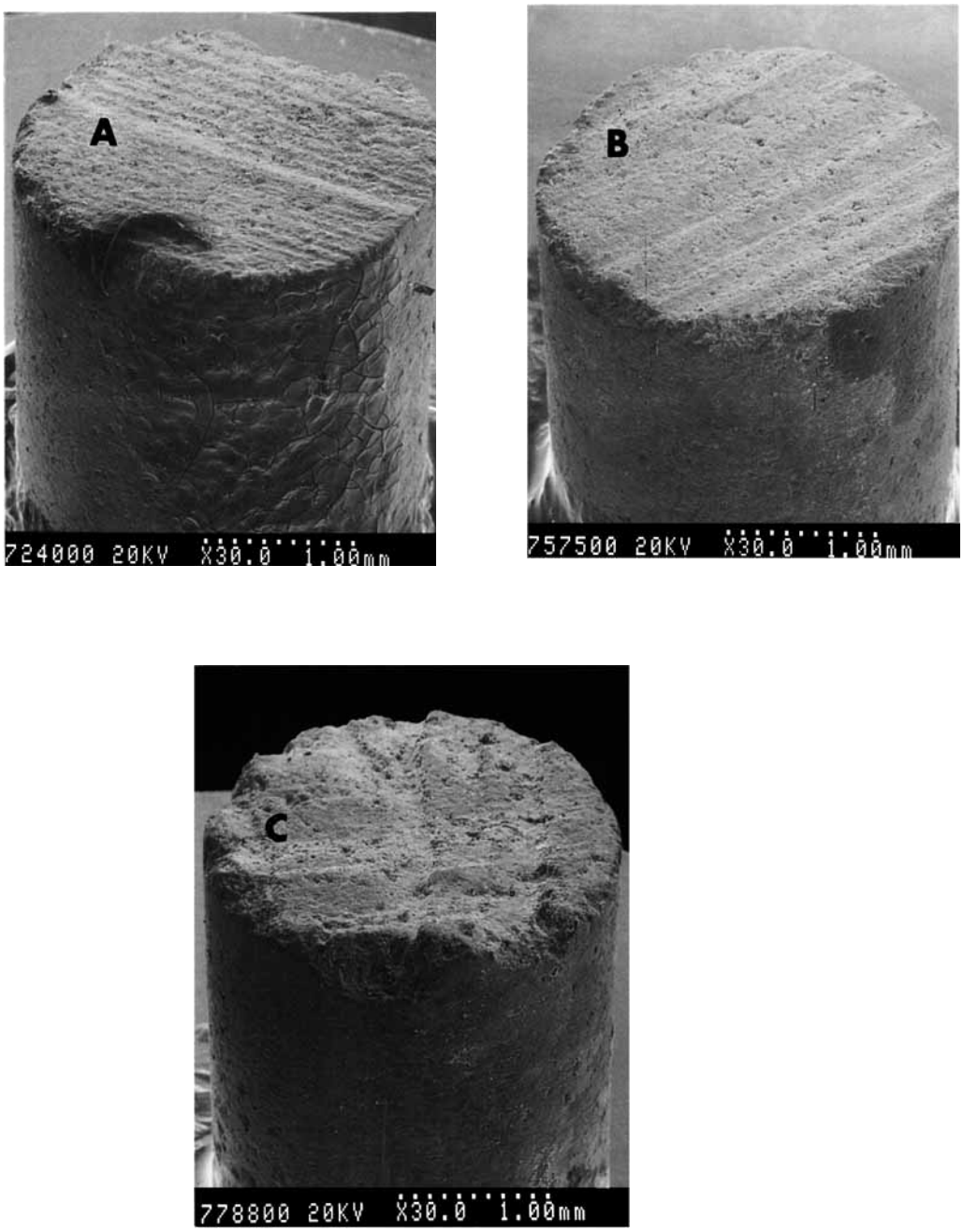

Figure 6(b) SEM pictures showing effect of solution pH on SMA polymer deposition. pH, magnification: (A) 4.0, 30×; (B) 7.5, 30×; (C) 8.8, 30×.

The cracks and pores on the surface of the SMA layer explain the kinetics of SMA deposition. As seen in Figure 3, SMA shows rapid increase in polymer deposition till about 3 min when the first layer formation is complete; beyond this, the increase in polymer deposition with time is small due to the diffusional deposition occurring only through the cracks and pores. In the case of EAA, only the first phase is seen where the polymer starts to form a monolayer on the particles and the complete coverage of the particles shows as an increase in polymer deposition with increase in time. Growth beyond this phase is, however, absent for EAA due to the nonporous nature of the film.

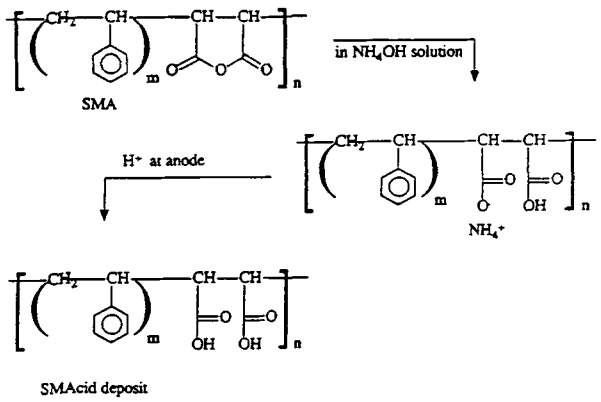

Figure 7 Mechanism of SMA polymer deposition.

Fourier Transform Infrared (FTIR) Spectroscopy

FTIR spectroscopic analyses were carried out on the deposited SMA films as well as on the original powder. Figure 8(a) shows a plot of % transmittance versus wave number for the original powder SMA while Figure 8(b) is for the deposited SMA. The band assignment[11-13] is given in Table I. The deposited and original SMA spectra differ in the region of 1100–950 cm^{-1} wavenumber. The two peaks seen here for the original SMA powder correspond to monosubstituted benzene ring, and are suppressed for the deposited SMA case.

Table I FTIR Band Assignments for SMA

No.	Band Wave Number (cm^{-1})	Possible Bond Assignment
1	2925	$-CH_2$
2	2890	$-CH$
3	2850	$-CH$
4	1790	$-O=C-O-C=O$
5	1700	$-C=O$
6	1590	$-\phi$
7	1500	$-\phi$
8	1460	$-CH_2$
9	1390	$-CH$
10	1220	$-\phi$
11	1085	$-\phi$
12	975	$-\phi$
13	930	$-C=O$
14	750	$-\phi-CH_2-CH_3$
15	680	$-\phi$

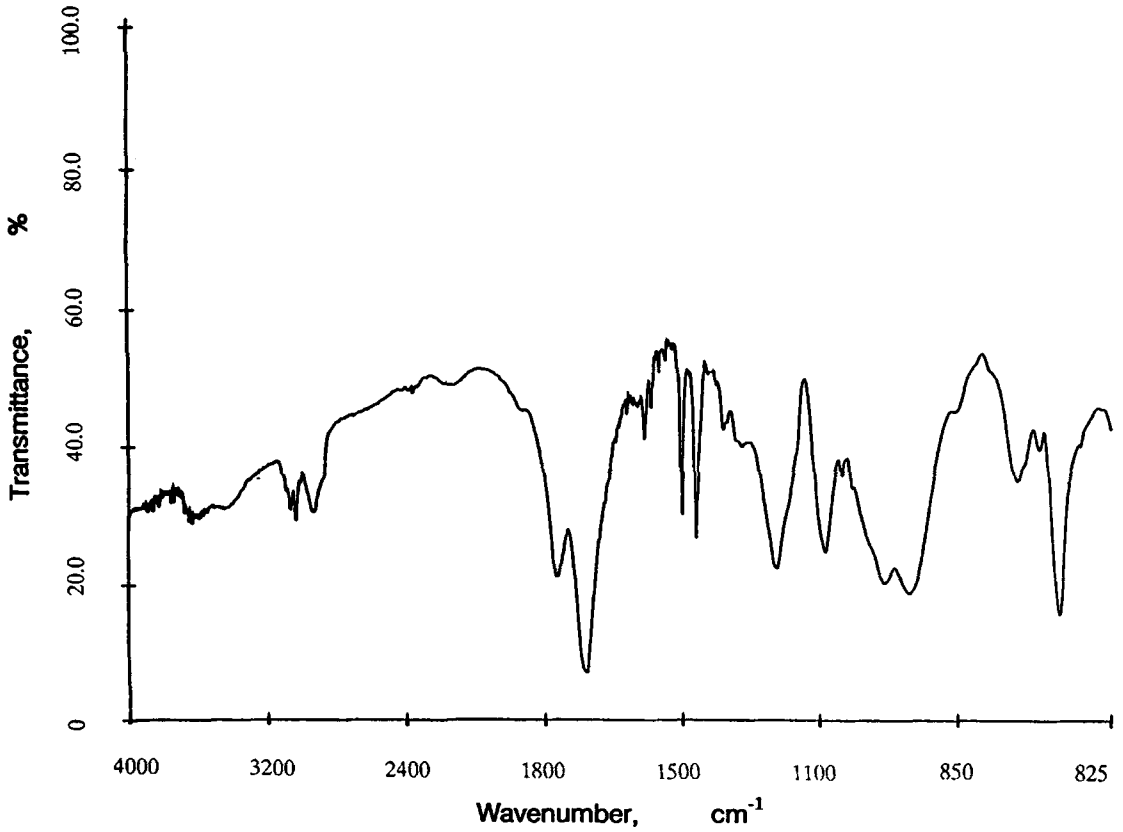

Figure 8(a) FTIR spectrum of original SMA polymer.

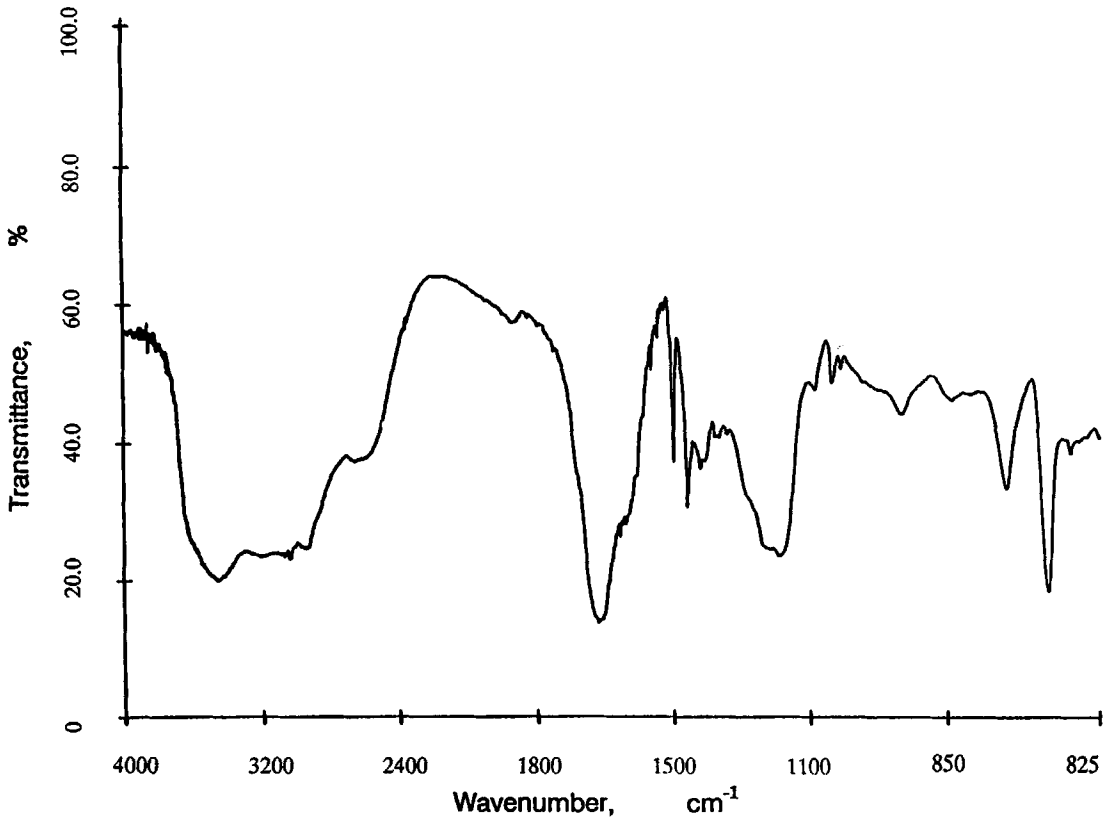

Figure 8(b) FTIR spectrum of deposited SMA polymer.

CONCLUSIONS

The SMA films obtained were porous, showed cracks on the surface, and were thick with multiple layers deposited. Thus, the SMA films showed both nucleation and growth phases. In the FEBR, the polymer film deposits were maximum at a feeder current of 0.2 A and showed a dual-peak behavior with increasing anolyte flow rate. The peaks occurred at incipient fluidization and at approximately 22.2% bed expansion (i.e., at a bed porosity of 0.648). Since the SMA polymer film deposits were nonconductive, they allowed a maximum deposition time of only 8 min at 0.2 A feeder current. The SMA polymer deposit was found to increase with increase in concentration of anolyte SMA and decrease with increase in pH of anolyte SMA.

Portions of this research were supported with funds from the National Science Foundation Grant #CBT-8519001.

REFERENCES

1. R. Mahalingam, F. S. Teng, and R. V. Subramanian, *J. Appl. Polym. Sci.*, **22**, 3587 (1978).
2. F. S. Teng, Ph.D. thesis, Chemical Engineering, Washington State University, Pullman, 1979.
3. F. S. Teng and R. Mahalingam, *Polym. Commun.*, **27**, 342 (1986).
4. F. S. Teng and R. Mahalingam, *J. Appl. Polym. Sci.*, **34**, 2837 (1987).
5. S. Segelke, M.S. thesis, Chemical Engineering, Washington State University, Pullman, 1988.
6. S. Segelke, R. Mahalingam, and R. V. Subramanian, *J. Appl. Polym. Sci.*, **40**, 297 (1990).
7. V. M. Desai, M.S. thesis, Chemical Engineering, Washington State University, Pullman, 1988.
8. V. M. Desai, R. Mahalingam, and R. V. Subramanian, *J. Appl. Polym. Sci.*, to appear.
9. A. E. Rheineck and A. M. Usmani, *Electrodeposition of Coatings*, Adv. in Chem. Ser. 119, Am. Chem. Soc., Washington, DC, 1973.
10. D. A. Olson, *J. Paint Technol.*, **38**, 429 (1966).
11. C. J. Pouchert, *The Aldrich Library of Infrared Spectra*, 3rd ed., Aldrich Chem. Co., 1981.
12. K. Nakanishi and P. H. Solomon, *Infrared Absorption Spectroscopy*, 2nd ed., Holden-Day, 1977.
13. J. H. van der Maas, *Basic Infrared Spectroscopy*, 2nd ed., Pitman, 1969.

Received October 22, 1990
Accepted February 7, 1991